Research Article

Journal of Physical Organic Chemistry

Received: 6 April 2007, Revised: 9 January 2008, Accepted: 10 January 2008, Published online in Wiley InterScience: 2008

(www.interscience.wiley.com) DOI 10.1002/poc.1345

Synthesis of novel bis(β-cyclodextrin)s linked with aromatic diamine and their molecular recognition with model substrates

Yan Zhao[a]*, Xiao-Qing Liu[a], Juan Gu[a], Li-Qin Wang[a], Hong-You Zhu[b], Rong Huang[c], Yu-Fei Wang[a] and Zi-Ming Yang[a]

Novel β-cyclodextrin (β-CD) dimers with aromatic diamine linkers, 1,3-(aminomethyl)-benzylamine-bridged bis(6-amino-6-deoxy-β-CD) (2), 4,4′-diaminodiphenylmethano-bridged bis(6-amino-6-deoxy-β-CD) (3), and 4,4′-ethylenedianiline-bridged bis(6-amino-6-deoxy-β-CD) (4), were synthesized. The inclusion complexation behaviors of these compounds, together with 4,4′-aminophenyl ethyl-bridged bis(6-amino-6-deoxy-β-CD) (5), with substrates such as acridine red (AR), neutral red (NR), ammonium 8-anilino-1-naphthalenesulfonate (ANS), sodium 2-(*p*-toluidinyl) naphthalenesulfonate (TNS), rhodamine B (RhB), and brilliant green (BG), were investigated by ultraviolet, fluorescence, circular dichroism, and 2D NMR spectroscopy. The results indicated that the two linked CD units cooperatively bound to a guest, and the molecular binding affinity toward substrates, especially curved guest ANS and linear guests such as NR and AR, was increased. The linker length between two CD units played a crucial role in the molecular recognition of the hosts with guest dyes. The binding constants of the hosts for AR, TNS, ANS, and RhB decreased with increasing linker length in hosts 2-4. Moreover, structurally similar hosts 3 and 5 exhibited very different binding behavior for the guests. Host 5 showed much higher *K*s values toward positively charged guests and lower *K*s toward negatively charged guests than host 3. The 2D NMR spectra of hosts 3 and 5 with RhB were acquired to understand the binding difference between 3 and 5. The molecular binding ability and selectivity of model substrates by these hosts were sufficiently investigated to reveal not only the cooperative contributions of the linker group and CD cavities upon inclusion complexation with dye guest molecules, but also the controlling factors for the molecular selective binding. Copyright © 2008 John Wiley & Sons, Ltd.

Keywords: bridged bis(β-CD)s; dyes; molecular recognition; cooperative binding mode; inclusion complexation

INTRODUCTION

The native and modified cyclodextrins (CDs) have been extensively used in chemical research and technology as artificial enzymes for biological mimicking.[1–6] Recent investigations have demonstrated that bis(β-CD)s bind better and more selectively with certain guest molecules than monomeric CDs,[7–14] and the improved properties of the modified CDs are attributed to the cooperative two-point recognition that mimics the highly substrate-specific binding of enzymes.[15–21] A variety of bis(β-CD)s with considerable structural diversity have been prepared to elucidate their complexation behavior as well as the factors and mechanisms governing the multipoint recognition upon inclusion complexation by bis(β-CD)s using various linkers such as alkanedioates,[22,23] disulfides,[24,25] dipyridines,[26–29] imidazole,[30,31] oligo (ethylene diamino),[32] and organoselenium.[33–37] However, synthetic and molecular recognition studies on aromatic diamino-bridged CD dimers are rare, except for recent studies by our group and Liu *et al.*[38–41] We have recently shown that aromatic diamino-bridged bis(β-CD)s form more stable complexes with the model substrates than the native β-CD through the cooperative binding of one guest molecule by two CD moieties. These results advanced our understanding of the several weak interactions in the multipoint recognition and induced-fit processes involving two adjacent receptor units (host) and a substrate molecular (guest) and prompted us to further investigate the inclusion complexation behavior of other aromatic diamino-bridged bis(β-CD)s.

In the present study, we chose aromatic diamino-bridged bis(β-CD)s as specific host molecules based on the consideration that the aromatic diamines not only enhance hydrophobicity of the microenvironment, but also adjust the dimension of the hydrophobic cavity of CD. We report the syntheses and molecular recognition behavior studies of aromatic diamino-bridged bis(β-CD)s (Scheme 1) with some representative organic dyes of different structures (Scheme 2) by fluorescence, ultraviolet, circular dichroism, and 2D NMR spectroscopy. We demonstrated that factors governing the cooperative binding of bis(β-CD)s

* *College of Chemistry and Chemical Engineering, Yunnan Normal University, Kunming 650092, China.*
E-mail: zhaooyann@163.com

a *Y. Zhao, X.-Q. Liu, J. Gu, L.-Q. Wang, Y.-F. Wang, Z.-M. Yang*
College of Chemistry and Chemical Engineering, Yunnan Normal University, Kunming 650092, China

b *H.-Y. Zhu*
School of Chemical Science and Technology, Yunnan University, Kunming 650091, China

c *R. Huang*
Experimental Center, Yunnan University, Kunming 650091, China

Journal of Physical Organic Chemistry

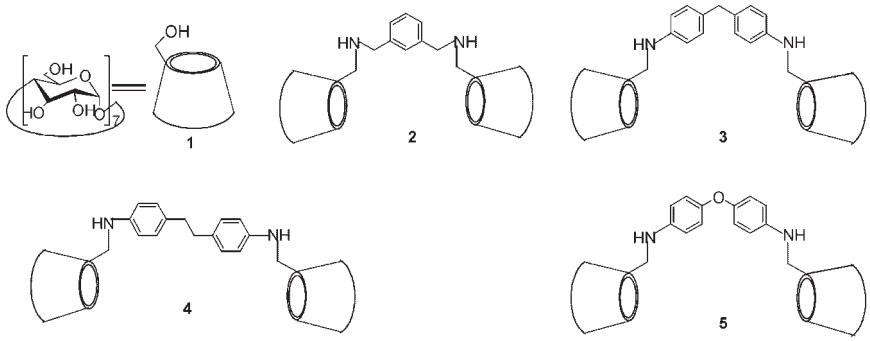

Scheme 1. Host structures

depended on not only the general size/shape fitting between the cavities of bis(β-CD)s and guest molecules, but also the structure, length, and flexibility of the linker.

EXPERIMENTAL

Materials

All guest dyes, including acridine red (AR), neutral red (NR), ammonium 8-anilino-1-naphthalenesulfonate (ANS), sodium 2-(*p*-toluidinyl) naphthalenesulfonate (TNS), rhodamine B (RhB) and brilliant green (BG), were obtained from commercial sources and used without further purification. β-CD of reagent grade (Shanghai Reagent Works) was recrystallized twice from water and dried under vacuum at 95 °C for 24 h prior to use. *N, N*-dimethylformamide (DMF) was dried over calcium hydride for 2 days and then distilled under reduced pressure. Mono[6-*O*-(*p*-toluenesulfonyl)]-β-CD was prepared from β-CD and *p*-toluenesulfonyl chloride in aqueous alkaline solution.[42] The phosphate buffer (0.10 mol · dm^{-3}, pH 7.20), used in the spectral measurements, was prepared from NaH_2PO_4 and Na_2HPO_4. 4,4′-Aminophenyl ethyl-bridged bis(6-amino-6-deoxy-β-CD) **(5)** was prepared as previously reported.[38]

Instruments and measurements

Combustion analyses were performed on an Elementar Vario EL III. ^{1}H NMR spectra were recorded on a Bruker AV. DRX5 instrument operated at 500 MHz. FT-IR spectra were obtained on a Bruker FL-IR. Circular dichroism and UV-vis spectra were recorded in a conventional quartz cell (light path 10 mm) on a JASCO 810 spectropolarimeter and a Shimadzu UV2401 PC spectrometer, respectively. Fluorescence spectra were measured in a conventional quartz cell ($10 \times 10 \times 45$ mm^3) at 25 °C on a Hitachi F-4500 spectrometer equipped with a constant-temperature water bath, with the excitation and emission slits of 10 nm width. The excitation wavelengths for AR, NR, ANS, TNS, and RhB were 490, 510, 350, 366, and 520 nm, respectively. In the fluorescence titration experiments, the concentration ranges of dyes and bis(β-CD)s were 1–10 and 30–480 μmol · dm^{-3}, respectively.

Synthesis

1, 3-(Aminomethyl)-benzylamine-bridged bis(6-amino-6-deoxy-β-CD) ***(2)***

As shown in Scheme 3, 1,3-(aminomethyl)-benzylamine (1.7 mmol, 0.23 g) and mono[6-*O*-(*p*-toluenesulfonyl)]-β-CD (4.0 mmol, 5.3 g) were dissolved in anhydrous DMF (40 mL), and the reaction mixture was stirred at 85–90 °C under nitrogen atmosphere for 3 days, followed by evaporation under reduced pressure to dryness. The residue was dissolved in a small amount of water, and the resultant solution was poured into acetone with vigorous stirring to obtain a brown-yellow precipitate. The crude product was collected by filtration and chromatographed on a Sephadex

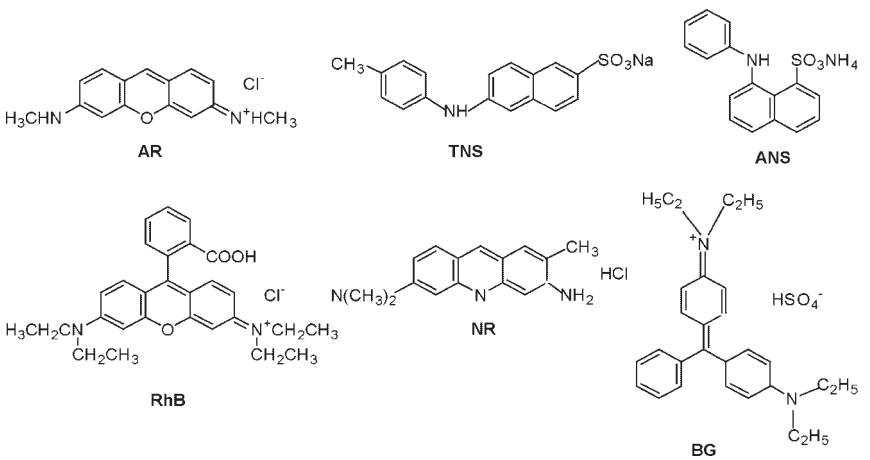

Scheme 2. Guests structures

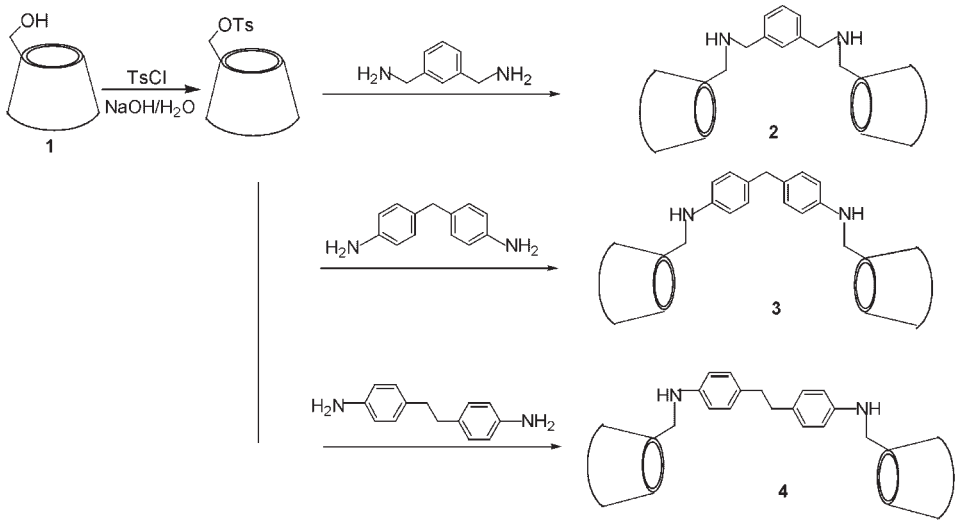

Scheme 3. Synthetic routes

G-25 column with water as eluent to give the pure sample **2** (0.43 g, yield 10%). FAB-MS: *m/z* 2371 ($M^+ + H$). ^{1}H NMR (D_2O, 500 MHz, TMS, ppm) δ: 2.7–2.9 (m, 4H), 3.4–3.9 (m, 84H), 4.9–5.0 (m, 14H), 7.1–7.5 (m, 4H). FT-IR (KBr) ν/cm^{-1}: 3490.1, 2927.3, 1704.6, 1659.4, 1416.6, 1337.7, 1231.7, 998.0, 934.1, 852.98, 807.7, 754.7, 689.47, 574.89. UV/vis (H_2O) λ_{max}/nm (ε/dm$^3 \cdot$ mol$^{-1} \cdot$ cm^{-1}) 260 (957), 219 (23438). Anal. calculated for $C_{92}H_{148}O_{68}N_2 \cdot 8H_2O$: C, 43.95; H, 6.57; N, 1.11. Found: C, 44.17; H, 6.39; N, 1.09.

4, 4′-Diaminodiphenylmethano-bridged bis(6-amino-6-deoxy-β-CD) ***(3)***

bis(β-CD) **3** was prepared similarly as **2** in 10% yield from 4,4′-diaminodiphenylmethane and mono[6-*O*-(*p*-toluenesulfonyl)]-β-CD as a yellowish solid. FAB-MS: *m/z* 2471 ($M^+ + K$). ^{1}H NMR (D_2O, 500 MHz, TMS, ppm) δ: 2.3–2.4 (s, 2H), 3.3–3.9(m, 84H), 4.9–5.0(m, 14H), 7.3(d, 4H), 7.6(d, 4H). FT-IR (KBr) ν/cm^{-1}: 3401.2, 2926.0, 1620.2, 1520.7, 1317.4, 1153.5, 1031.1, 938.2, 856.6, 754.7, 701.7, 578.7, 522.3, 436.7. UV/vis (H_2O) λ_{max}/nm (ε/dm$^3 \cdot$ mol$^{-1} \cdot$ cm^{-1}) 202(51765), 252(25984). Anal. calculated for $C_{97}H_{150}O_{68}N_2 \cdot 6H_2O$: C, 45.86; H, 6.43; N, 1.10. Found: C, 45.44; H, 6.36; N, 1.11.

4, 4′-Ethylenedianiline-bridged bis(6-amino-6-deoxy-β-CD) ***(4)***

bis(β-CD) **4** was similarly as **2** prepared in 9% yield from 4,4′-ethylenedianiline and mono[6-*O*-(*p*-toluenesulfonyl)]-β-CD as a yellowish solid. FAB-MS: *m/z* 2447 ($M^+ + H$). ^{1}H NMR (D_2O, 500 MHz, TMS, ppm) δ: 2.2–2.4 (m, 4H), 3.2–4.0(m, 84H), 4.9–5.0(m, 14H), 7.2(d, 4H), 7.5(d, 4H). FT-IR (KBr) ν/cm^{-1}: 3389.9, 2925.9, 2356.63, 1708.7, 1659.9, 1619.0, 1521.6, 1415.2, 1368.1, 1154.9, 1031.1, 930.0, 852.6, 756.2, 577.5. UV/vis (H_2O) λ_{max}/nm (ε/dm$^3 \cdot$ mol$^{-1} \cdot$ cm^{-1}) 202(28692), 228(13149). Anal. calculated for $C_{98}H_{152}O_{68}N_2 \cdot 16H_2O$: C, 43.04; H, 6.78; N, 1.02. Found: C, 43.52; H, 6.48; N, 1.06.

RESULTS AND DISCUSSION

Inclusion complexation stoichiometry

The stoichiometry for the inclusion complexation of bridged bis(β-CD)s with representative guests, that is, TNS, ANS, AR, NR, RhB, and BG was determined by the continuous variation method. The continuous variation plot for **4**/AR system is illustrated in Fig. 1. In the concentration range studied, the plot for bis(β-CD)s unit peaked at a molar fraction of 0.5, suggesting a 1:1 inclusion complexation between host and guest. The same results were obtained with other bis(β-CD)-host combinations (not shown).

Circular dichroism spectra

Circular dichroism spectrometry has become a convenient and widely employed method for the elucidation of the absolute conformation of chiral organic compounds in the past three decades.[43] Moreover, achiral compounds can also show the induced circular dichroism (ICD) signal in the corresponding transition band in cases where there is a chiral microenvironment. With an inherent chiral cavity, CDs can certainly provide such a microenvironment for the pendant group of the cavity. In this context, the circular dichroism spectra of bridged bis(β-CD)s **2**–**5** were measured in a dilute phosphate buffer (pH 7.20) to examine their original conformation. As shown in Fig. 2, hosts **2**–**5** displayed obviously different circular

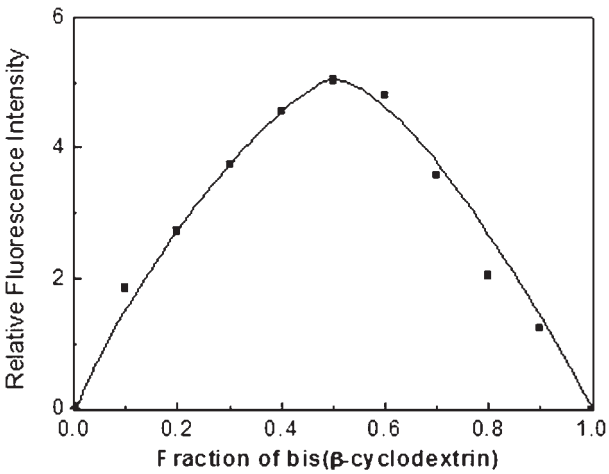

Figure 1. Continuous variation plot of **4**/AR system. ([bis(β-CD) unit] + [AR] = 2.0×10^{-5} mol $\cdot$ dm^{-3})

Journal of Physical Organic Chemistry

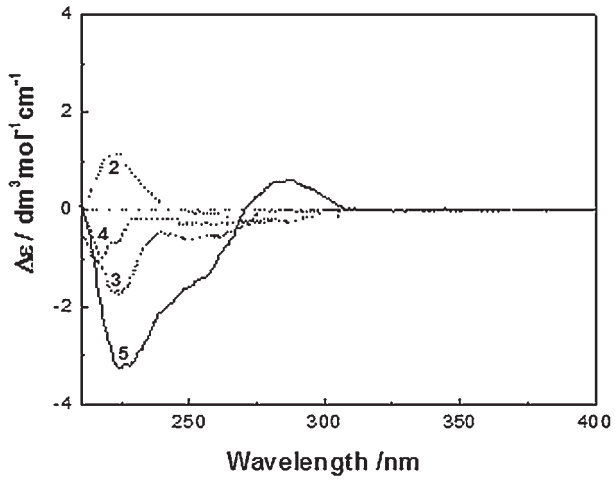

Figure 2. Circular dichroism spectra of bis(β-CD)s **2**–**5** (1.0×10^{-4} mol · dm^{-3}) in phosphate buffer (pH 7.20) at 25 °C

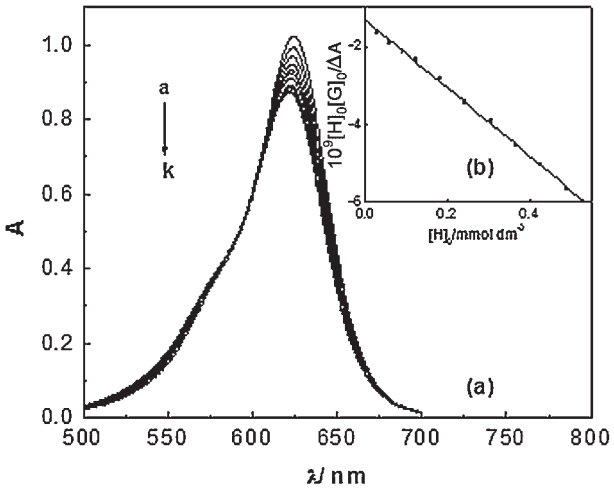

Figure 3. (a) UV-vis spectral changes of BG ($1.8\ \mu$mol · dm^{-3}) upon addition of host **2** in phosphate buffer (pH 7.20) at 25 °C; the concentration of host **2** (from a to k): 0, 30, 60, 90, 120, 180, 240, 300, 360, 420, 480 μmol · dm^{-3}, respectively. (b) Typical plots of $[H]_0[G]_0/\Delta A$ *versus* $[H]_0$ for the inclusion complexation of host **2** with BG in phosphate buffer (pH 7.20) at 25 °C

dichroism spectra in the absence of a guest, indicating the differences in the interactions between the aromatic linker and two chiral cavities in these compounds. Bis(β-CD) **2** exhibited a moderate positive Cotton effect peak ($\Delta\varepsilon = +1.15$ dm^{-3} · mol^{-1} · cm^{-1}) at 226 nm and a weak negative Cotton effect peak ($\Delta\varepsilon = -0.28$ dm^{-3} · mol^{-1} · cm^{-1}) at 277 nm, attributed to the ^1L_a band and ^1L_b band, respectively. The bridged bis(β-CD)s **3** and **4**, possessing similar linkers, displayed very similar patterns on the circular dichroism spectra. Both showed two negative Cotton effect peaks, corresponding to the ^1L_a and ^1L_b bands of the phenyl chromophores. The $\Delta\varepsilon$ values (in dm^{-3} · mol^{-1} · cm^{-1}) were −1.72 at 222 nm and −0.56 at 262 nm for the ^1L_a and ^1L_b band of **3**, respectively; −0.99 at 218 nm and −0.30 at 271 nm for the ^1L_a and ^1L_b band of **4**, respectively. Interestingly, substitution of the methylene group between two benzene groups in the linker of bis(β-CD) **3** with an oxygen atom resulted in the strongest ICD signals as observed with **5**, a strong negative Cotton effect peak around 225 nm (−3.27 dm^{-3} · mol^{-1} · cm^{-1}) and a weak positive Cotton effect peak around 287 nm (+0.61 dm^{-3} · mol^{-1} · cm^{-1}) for the ^1L_a and ^1L_b transitions, respectively. According to the empirical rule proposed by Kajtar,[44] Harata,[45] and Kodaka,[46] we propose that the benzene ring in host **5** might shallowly penetrate into the β-CD cavity, while the oxygen atom in the linker might be in close contact with the cavity, which could lead to stronger hydrogen bond interactions with the outside hydroxy groups of the β-CD. However, the benzene ring in the linker of **2**, **3**, and **4** just shallowly perched over the rim of the β-CD cavity. Both ^1L_a and ^1L_b transition moments of **3** and **4** were nearly perpendicular to the CD axis, resulting in the two negative Cotton effect peaks.

Fluorescence titration

Spectral titrations of bis(β-CD)s with structurally related dye guests were performed at 25 °C in phosphate buffer (pH 7.20) to quantitatively assess the inclusion complexation behavior of these compounds. The fluorescence intensities of guest molecules, especially ANS and TNS, were relatively weak, but the stepwise addition of the host compound caused significant successive enhancement in fluorescence intensity with appreciable hypsochromic shifts. The hypsochromic shift of the fluorescence peak for AR was relatively small compared with NR, RhB, ANS, and TNS. These observations suggested that the guest molecules were shifted from the bulk water outside the cavity toward the interior of the hydrophobic cavity, resulting in increased hydrophobicity of the microenvironment around guest molecules. To further investigate the molecular binding ability and selectivity, the binding constants of bis(β-CD)s with BG were determined by ultraviolet spectroscopy. Fig. 3a shows the spectral changes of BG with gradual addition of host **3**. As shown in Fig. 3a, the intensity at the absorption maximum around 625 nm of BG decreased considerably with the increase of the concentration of host **3**, indicating the formation of the inclusion complex between host **3** and BG.

By treating one bis(β-CD) moiety in hosts **2**–**5** as a host unit, the inclusion complexation of guest (*G*) with host (*H*) is expressed by Eqn 1 and the complex stability constant (*Ks*) is given by Eqn 2.

$$H + G \overset{K_s}{\rightleftharpoons} G \cdot H \tag{1}$$

$$K_S = \frac{[H \cdot G]}{[H][G]} \tag{2}$$

$$\Delta A = \Delta\varepsilon[H \cdot G] \tag{3}$$

where ΔA and $\Delta\varepsilon$ denote the sequential changes of absorption and the differential molar extinction coefficient of dye guest in the absence and presence of bis(β-CD). Under the conditions employed, the initial concentration of the bis(β-CD)s is much larger than that of guest molecules, that is, $[H]_0 >> [G]_0$. Therefore, the combination of Eqns 2 and 3 leads to the extended Benesi–Hildebrand equation (Eqn 4), which is used to calculate the complex stability constants (*Ks*) (Eqn 2) from the slope and intercept of $[H]_0[G]_0/\Delta A$ *versus* $[H]_0$ plots.

$$\frac{[H]_0[G]_0}{\Delta A} = \frac{1}{K_s \Delta A} + \frac{[H]_0}{\Delta A} \tag{4}$$

Table 1. Complex stability constant (*Ks*) and Gibbs free energy change ($-\Delta G^{\circ}$) for 1:1 inclusion complexation of dye guests with β-CD **1** and bis(β-CD)s **2**–**5** in aqueous buffer solution (pH 7.20) at 25 °C

Host	Guest	λ^{F}_{max}/nm[a]	*Ks*	Log *Ks*	$-\Delta G$ (kJ mol^{-1})	Methods[b]	Ref.
1	AR	552	2630	3.42	19.5	FL	[52]
	NR	576	480	2.68	15.3	FL	This work
	ANS	515	103	2.01	11.5	FL	[53]
	TNS	475	3670	3.56	20.3	FL	[53]
	RhB	572	4240	3.63	20.7	FL	[52]
	BG	—	2187	3.34	19.1	UV	[32]
2	AR	551	26 700	4.43	25.3	FL	This work
	NR	566	2409	3.38	19.3	FL	This work
	ANS	509	3418	3.53	20.1	FL	This work
	TNS	469	10 358	4.02	22.9	FL	This work
	RhB	567	16 780	4.22	24.1	FL	This work
	BG	—	6558	3.82	21.8	UV	This work
3	AR	550	10 272	4.01	22.9	FL	This work
	NR	564	6875	3.84	21.9	FL	This work
	ANS	509	2654	3.42	19.5	FL	This work
	TNS	467	7091	3.85	22.0	FL	This work
	RhB	568	8367	3.92	22.4	FL	This work
	BG	—	11 872	4.07	23.2	UV	This work
4	AR	552	8711	3.94	22.5	FL	This work
	NR	565	8889	3.95	22.5	FL	This work
	ANS	507	1847	3.27	18.7	FL	This work
	TNS	469	5841	3.77	21.5	FL	This work
	RhB	568	7405	3.87	22.1	FL	This work
	BG	—	9534	3.98	22.7	UV	This work
5	AR	553	17 616	4.25	24.3	FL	[38]
	NR	567	7548	3.87	22.1	FL	[38]
	ANS	510	1653	3.22	18.4	FL	This work
	TNS	468	5934	3.77	21.5	FL	This work
	RhB	568	6432	3.81	21.7	FL	This work
	BG	—	18 475	4.27	24.4	UV	This work

[a] Ultimate maximum fluorescence wavelength obtained upon addition of large excess of host, while the λ^{F}_{max}/nm of AR, NR, ANS, TNS, and RhB are 559, 598, 522, 418, and 572 nm, respectively.
[b] Fl: fluorescence, UV: Ultraviolet/Visible.

Figure 3b illustrates the result of such a treatment for the inclusion complexation of host **3** with BG, where the calculated $[H]_0[G]_0/\Delta A$ values were plotted against the $[H]_0$ values, generating an excellent linear curve. The complex stability constants (*Ks*) and the free energy changes ($-\Delta G^{\circ}$) calculated from the slope and intercept are listed in Table 1.

Binding mode

The bis(β-CD)s exhibited higher K_S values toward dye guests than the native β-CD (Table 1), which might be attributed to the cooperative binding of two adjacent CD cavities and the potential multiple recognition behavior of such compounds. The native or mono-modified CDs generally encapsulate the guest molecules into the cavities from the wide openings to minimize the interactions with water and/or decrease steric hindrance. Comparing with the mono-modified CDs, the bridged bis(β-CD)s, which are connected from not only the primary but also the secondary sides, can significantly enhance their molecular binding ability and selectivity through the cooperative binding of two CD cavities with one guest molecule and the formation of a sandwich-type host–guest complex.[18,47–51] To further investigate the inclusion complexation behavior and deduce the molecular recognition mechanism of dye guests by these aromatic diamino-bridged bis(β-CD)s, 2D NMR spectra were obtained for hosts **3** and **5** with RhB in D_2O. Fig. 4a and b show the ^{1}H NOESY spectra of hosts **3** and **5** in the presence of guest RhB, respectively, with three clear NOE cross-peaks labeled as peak A, B, and C. Peak A indicated the interaction between the H-3 and H-5 (comparable intensities) of the CD and the methyl protons of diethylamino fragments in RhB, suggesting that the methyl protons of the diethylamino groups were inserted from the primary side of CD and deeply embedded in the cavities of CD. The cross-peaks between H-3 (weak) and H-5 of CD and the aromatic protons of diethylaminophenyl groups in RhB, and the cross-peaks between the aromatic protons on the aromatic

Journal of Physical Organic Chemistry

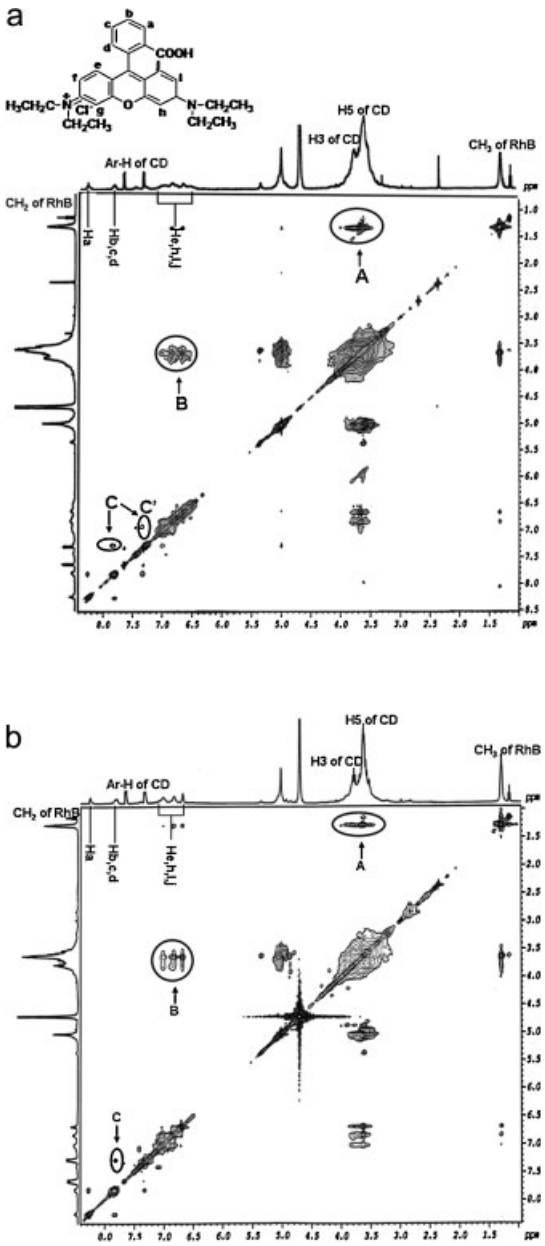

Figure 4. ^{1}H NOESY spectra of hosts **3** (a) and **5** (b) in the presence of RhB in D_2O ([Host] = [RhB] = 5.0×10^{-3} mol · dm^{-3}) with a mixing time of 600 ms at 298 K

diamine linker of hosts **3** and **5** and the aromatic protons of the benzoate moiety in RhB, were labeled as peak B and peak C, respectively. Peaks A, B, and C of host **3** were of greater intensities than those of host **5**, suggesting a more stable binding of host **3** with RhB, which is consistent with the results obtained by spectral titration. In addition, the unique peak C′ of host **3** was the cross-peak between the aromatic protons on the aromatic diamine linker of host **3** and the aromatic protons of diethylaminophenyl groups in RhB. This implies that the aromatic diamine linker of host **3** made more contribution in the binding process with RhB than that of host **5**. Based on all these results, we propose a possible multiple binding mode in the complexation of RhB by bis(β−CD) as shown in Fig. 5. In this mode, two diethylaminophenyl groups of RhB were included in the hydrophobic CD cavities from the narrow side to form a 'face-to-face' sandwich inclusion complex, while the benzoate branch of RhB was located partially or entirely in the pseudocavity formed by the linker groups of hosts. Thus, the guest molecule was more efficiently shielded from the attack of solvent water by the cooperative inclusion complexation with CD cavities and the formation of the sandwich host–guest complex. Additionally, under our experimental condition at pH 7.20, the carboxyl group of RhB in aqueous solution was not protonated and existed as a carboxylate anion and the —NH— group in the linker of bis(β-CD) should be partially protonated. We postulate that the negatively charged benzoate component of RhB should penetrate into the pseudo cavity of bis(β-CD) to interact with the positively charged —NH_2^+— in the linker.

Molecular binding ability and molecular selectivity

It has been widely reported that the functional linker between two CD units plays a crucial role in determining the host–guest binding abilities in the molecular multiple recognition of bis(β-CD)s. The conformation, length, and flexibility of the linker can control how the CD cavities adjust their orientation and distance to cooperatively bind one guest molecule through the simultaneous operation of several weak forces, such as ion–dipole, dipole–dipole, dipole–induced dipole, van der Waals, electrostatic, hydrogen bonding, and hydrophobic interactions. The complex stability constants (*K*s) of bis(β-CD)s **2**–**5** with the guest molecules are obviously larger than those of native β-CD (Table 1). As a result of cooperative binding, the bridged bis(β-CD) **2** exhibited the highest enhancement factor for ANS at 33.2. The importance of guest structure was more clearly demonstrated by comparing the effect of the bis(β-CD)s on each guest. The bis(β-CD)s host that gave the highest enhancement for each guest dye (with the observed enhancement factors shown in the parentheses) was: **2** (×10.2) for AR, **4** (×18.5) for NR, **2** (×33.2) for ANS, **2** (×2.8) for TNS, **2** (×4.0) for RhB and **5** (×8.4) for BG. By comparing the enhancement factors, we concluded that the curved guest ANS and linear guests NR and AR were more capable of cooperatively binding bis(β-CD)s than the linear guest TNS, the triangular BG and T-shaped RhB.

Moreover, further comparison of the structures of the examined dye molecules shows that these guest molecules share some structural and functional similarities. For instance, both AR and NR possess a heterocycle anthracene moiety. Compared with the parent β-CD **1**, bridged bis(β-CD)s **2**–**5** formed much more stable inclusion complexes with AR and NR through cooperative binding by two CD units, displaying a binding affinity sequence of AR > NR, except for host compound **4**. However, the effect of the cooperative binding by bis(β-CD)s was more remarkable for NR, showing a higher binding constant upon inclusion complexation with hosts **2**–**5**. This indicates that, although AR and NR possess similar residues, they exhibit dramatically different complexation behavior with the hosts. The guest AR with a small substituent could be well embedded in the cavity of β-CD **1** in the longitudinal direction, and the second cavity in the dimeric hosts **2**–**5** merely enhanced the *K*s value by 3.3–10.2 times. On the other hand, the guest NR could only partially penetrate into the cavity of β-CD **1** to form a weaker inclusion complex due to steric hindrance. Therefore, the contribution of the second cavity in hosts **2**–**5** was much greater

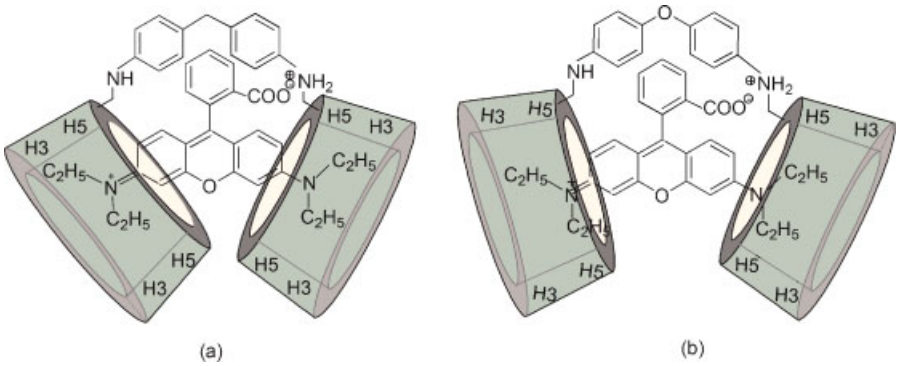

Figure 5. Possible inclusion binding modes of (a) host **3** with RhB and (b) host **5** with RhB. This figure is available in color online at www.interscience.wiley.com/journal/poc

and it enhanced the *K*s values by a factor of 5.0–18.5 for NR. It was also noted that, although all hosts examined formed less stable complex with ANS than with TNS, the enhanced molecular binding affinity by the cooperative binding of bis(β-CD)s for ANS was more remarkable than that for TNS. The enhancement factors for ANS, 33.2 (**2**), 25.8 (**3**), 17.9 (**4**), and 16 (**5**), were much higher than those for TNS, 2.8 (**2**), 1.9 (**3**), 1.6 (**4**), and 1.6 (**5**). These results further demonstrated that the size and shape of guest molecules were very important factors for enhancing the binding affinity of bridged bis(β-CD)s.

bis(β-CD)s not only promoted the guest binding in most cases, but also enhanced the guest selectivity through multipoint recognition and fine tuning of the orientation of the host and the linker. The enhancement of molecular selectivity of bis(β-CD) **2** for AR/ NR was 2.0 times that of the parent β-CD. Moreover, a close examination of the molecular binding affinity toward the BG/RhB pair revealed that the linker length between two CD units affected the molecular selectivity. For example, the native β-CD **1** and bis(β-CD) **2** with a short linker showed relatively good molecular selectivity up to 1.9 and 2.6, respectively, for the RhB/ BG pair. But bis(β-CD)s **3**, **5** with moderate length linkers and **4** with a long linker exhibited the opposite molecular selectivity, yielding the BG/RhB selectivity of 1.4, 2.9, and 1.3, respectively.

It was interesting to compare the 'host selectivity' sequence obtained for six guest dyes. The *K*s value for the complexation of each dye by native β-CD **1** and bis(β-CD)s **2**–**4** increased in the order:

AR: **2** > **3** > **4** > **1**
NR: **4** > **3** > **2** > **1**
TNS: **2** > **3** > **4** > **1**
ANS: **2** > **3** > **4** > **1**
RhB: **2** > **3** > **4** > **1**
BG: **3** > **4** > **2** > **1**

There was a general tendency in the binding constants for AR, TNS, ANS, and RhB, to decrease with increasing linker length in hosts **2**-**4**, that is, the binding constants of bridged bis(β-CD)s linked by a rigid linker was larger than that with a flexible linker. Host **2** displayed the highest binding affinity among the four dimeric CDs for AR, TNS, ANS, and RhB guests. Its short and less flexible linker was probably responsible for this high binding affinity. This effect of linker length was entropy controlled because the cooperative effect was gradually decreased when the distance between two CD moieties was increased. However, the binding constants for BG and NR did not always decrease with the increase of the linker length. These results indicated that the match of size and shape between the host and the guest are critical for the stability of the inclusion complex. In this context, the linker length of host **3** was suitable for the cooperative binding of BG, while host **4** formed the most stable complex with NR. It is clear that many factors, including guest shape, the distance, and contacting surface area between host bis(β-CD)s and guest dyes, determine the host–guest selectivity.

It was interesting that the structurally similar hosts **3** and **5** displayed completely different binding behavior with guest molecules. As shown in Table 1, host **5** effectively enhanced the binding affinity of β-CD for positively charged guests such as AR, NR, and BG by 6.7, 15.7, and 8.4-fold, respectively. However, host **3** only displayed 3.9, 14.3, and 5.4-fold increases, respectively. Host **3** was more effective than host **5** in binding the negatively charged guests such as TNS, ANS, and RhB. Compared with the native β-CD, the binding constants of host **3** with TNS, ANS, RhB were increased by factors of 1.9, 25.8, and 2.0, and the *K*s values of host **5** were increased by factors of 1.6, 16.0, and 1.5, respectively. One possible explanation is that the oxygen atom in the linker of host **5** had higher electron density and provided some Lewis base characteristics compared with the methylene group in the linker of host **3**. The electrostatic interaction between the oxygen atom in the linker of host **5** with charged guests could affect the host–guest binding behavior too. Consequently, host **5** displayed a preference for charge recognition over shape recognition and showed a selectivity order of BG > AR > NR > RhB > TNS > ANS. As the aromatic linker of **5** likely penetrated into the cavity shallowly, the oxygen atom in the linker came in close contact with the cavity. The binding affinities of host **5** with cationic linear guests, such as AR and NR, were therefore enhanced through electrostatic attraction, van der Waals and/or hydrophobic interactions. In contrast, the electrostatic repulsion between the oxygen atom in the aromatic linker of **5** and the anionic linear guest TNS and curved guest ANS hindered the penetration of the guest into the CD cavity, resulting in poor host–guest inclusion. Since NR and ANS likely only partially penetrated into the CD cavity due to steric hindrance, and AR and TNS were likely fully trapped in the CD cavity from the longitudinal direction, host **5** formed more stable complex with AR and TNS than with NR and

ANS. Furthermore, host **5** showed the strongest binding affinities toward triangular BG among cationic guests and toward T-shaped RhB among anionic guests. This observation might be attributed to the affinity of the linker group of host **5** to form a well-organized pseudo cavity, which in turn provided additional binding interaction with the branch fragment of BG and RhB by forming a sandwich inclusion complex. The NOESY result appeared to suggest that the electrostatic, van der Waals, and/or hydrophobic interactions of host **5** with BG or RhB probably drove out the self-included phenyl moiety from CD cavity. An electrostatic interaction between the oxygen atom in the linker of host **5** and the ammonium group of BG or the carboxyl group of RhB may be accommodated in the pseudocavity, resulting in a more stable complex with BG than with RhB. All the results indicated that host **5** showed good molecular selectivity up to 2.3, 3.6, and 2.9 for the AR/NR, TNS/ ANS, and BG/RhB pair, respectively. However, host **3** gave the general selectivity of 1.5, 2.7, and 1.4, respectively. Also, the results showed that the oxygen atom introduced to the aromatic diamine linker not only affected the spatial relationship of two β-CD cavities, but also acted as an additional recognition site through electrostatic interaction giving higher *K*s values toward the positively charged guests than those of the negatively charged guests.

CONCLUSION

In conclusion, bridged bis(β-CD)s linked by aromatic diamine significantly increased the molecular binding affinity of the parent β-CD. The complex stability constants for the selected guests were 1.6–33.2 times larger than those of the native β-CD through cooperative interactions. The complex stability depended greatly on the conformation, length, flexibility of the aromatic diamine linker, structural features of bis(β-CD)s and the size/shape/charge of guests. The functional linkers linking two CD cavities also significantly affected the molecular selectivity of the hosts. This concept may be extended to other synthetic supramolecular systems and applied to the design and synthesis of new functional supramolecular species.

Acknowledgements

We thank Dr David Konkin, NRC Plant Biotechnology Institute (NRC-PBI), National Research Council of Canada, for his helpful comments on improving the manuscript. This work was supported by the Natural Science Foundation of Yunnan Province (Grant No. 2003C009M) and Grant for Scientific Research from Yunnan Provincial Department of Education (Grant No. 07Y10175), which was gratefully acknowledged.

REFERENCES

[1] R. Breslow, S. D. Dong, *Chem. Rev.* **1998**, *98*, 1997–2012.
[2] J. Szejti, *Chem. Rev.* **1998**, *98*, 1743–1754.
[3] P. L. Dentuto, L. Catucci, P. Cosma, P. Fini, A. Agostiano, L. D'Accolti, C. C. Trevithick-Sutton, C. S. Foote, *J. Phys. Chem. B* **2005**, *109*, 1313–1317.
[4] Y. Zhao, L. Li, Y. Liu, *Gaodeng Xuexiao Huaxue Xuebao (Chem. J. Chin. Univ.)* **2002**, *23*, 2272–2277 (in Chinese) [CAN 138: 271211].
[5] Y. Zhao, Z.-M. Yang, Z.-Y. Li, B.-Y. Li, F. A, X.-J. Bi, F. Ali, *Wuji Huaxue Xuebao (Chin. J. Inorg. Chem.)* **2006**, *22*, 679–684 (in Chinese) [CAN 145: 397017].
[6] Y. Zhao, X.-Q. Liu, Y. Zhao, P. Liu, C. Li, *Fenxi Huaxue Xuebao (Chin. J. Anal. Chem.)* **2006**, *34*, 959–962 (in Chinese) [AN 2007: 103236].
[7] R. Breslow, S. Halfon, B. Zhang, *Tetrahedron.* **1995**, *51*, 377–388.
[8] R. Breslow, Z. Yang, R. Ching, G. Trojandt, F. Odobel, *J. Am. Chem. Soc.* **1998**, *120*, 3536–3537.
[9] S. D. P. Baugh, Z. Yang, D. K. Leung, D. M. Wilson, R. Breslow, *J. Am. Chem. Soc.* **2001**, *123*, 12488–12494.
[10] J. J. Michels, J. Huskens, D. N. Reinhoudt, *J. Am. Chem. Soc.* **2002**, *124*, 2056–2064.
[11] M. R. De Jong, J. F. J. Engbersen, J. Huskens, D. N. Reinhoudt, *Chem. Eur. J.* **2000**, *6*, 4034–4040.
[12] M. R. De Jong, M. A. R. Knegtel, P. D. J. Grootenhuis, J. Huskens, D. N. Reinhoudt, *Angew. Chem. Int. Ed.* **2002**, *41*, 1004–1008.
[13] F. Venema, A. E. Rowan, R. J. M. Nolte, *J. Am. Chem. Soc.* **1996**, *118*, 257–258.
[14] F. Venema, H. F. M. Nelissen, P. Berthault, N. Birlirakis, A. E. Rowan, M. C. Feiters, R. J. M. Nolte, *Chem. Eur. J.* **1998**, *4*, 2237–2250.
[15] S. H. Chiu, D. C. Myles, R. L. Garrell, J. F. Stoddart, *J. Org. Chem.* **2000**, *65*, 2792–2796.
[16] J. M. Yan, R. Breslow, *Tetrahedron Lett.* **2000**, *41*, 2059–2062.
[17] J. M. Benito, M. G. Garcia, C. O. Mellet, I. Baussanne, J. Defaye, J. M. G. Ferna'ndez, *J. Am. Chem. Soc.* **2004**, *126*, 10355–10363.
[18] R. Breslow, B. Zhang, *J. Am. Chem. Soc.* **1996**, *118*, 8495–8496.
[19] D. K. Leung, Z. W. Yang, R. Breslow, *Proc. Natl Acad. Sci. USA* **2000**, *97*, 5050–5053.
[20] Y. Liu, Y.-L. Zhao, Y. Chen, F. Ding, G.-S. Chen, *Bioconjugate Chem.* **2004**, *15*, 1236–1245.
[21] Y. Liu, Y.-W. Yang, Y. Song, H.-Y. Zhang, F. Ding, T. Wada, Y. Inoue, *ChemBioChem.* **2004**, *5*, 868–871.
[22] R. Breslow, B. Zhang, *J. Am. Chem. Soc.* **1992**, *114*, 5882–5883.
[23] R. Breslow, N. Greenspoon, T. R. Guo Zarzycki, *J. Am. Chem. Soc* **1989**, *111*, 8296–8297.
[24] R. Breslow, S. Chuang, *J. Am. Chem. Soc.* **1990**, *112*, 9659–9660.
[25] Y. Okabe, H. Yamamura, K. Obe, K. Ohta, M. Kawai, K. Fujita, *J. Chem. Soc. Chem. Commun.* **1995**, 581–582.
[26] R. Deschenaux, T. Ruch, P. F. Deschenaux, A. Juris, A. Ziessel, *Helv. Chim. Acta* **1995**, *78*, 619–628.
[27] H. F. M. Nelissen, A. F. J. Schut, F. Venema, M. C. Feiters, R. J. M. Nolte, *J. Chem. Soc. Chem. Commun.* **2000**, 577–578.
[28] Y. Liu, X.-Q. Li, Y. Chen, X.-D. Guan, *J. Phys. Chem. B* **2004**, *108*, 19541–19549.
[29] Y. Liu, Y. Chen, L. Li, H.-Y. Zhang, S.-X. Liu, X.-D. Guan, *J. Org. Chem.* **2001**, *66*, 8518–8527.
[30] R. Breslow, S. Halfon, *Proc. Natl Acad. Sci. USA* **1992**, *89*, 6916–6918.
[31] M.-M. Luo, R.-G. Xie, D.-Q. Yuan, W. Lu, P.-F. Xia, H.-M. Zhao, *Chin. J. Chem.* **1999**, *17*, 384–390.
[32] Y. Liu, C.-C. You, B. Li, *Chem. Eur. J.* **2001**, *7*, 1281–1288.
[33] Y. Liu, L. Li, H.-Y. Zhang, Y. Song, *J. Org. Chem.* **2003**, *68*, 527–536.
[34] Y. Liu, L. Li, Y. Chen, *J. Inclusion Phenom. Macrocyclic Chem.* **2002**, *42*, 151–155.
[35] J.-Q. Liu, Y.-G. Ning, C.-B. Shi, G.-M. Luo, G.-C. Yan, J.-C. Shen, *Gaodeng Xuexiao Huaxue Xuebao (Chem. J. Chin. Univ.)* **1998**, *19*, 1446–1448 (in Chinese) [CAN 129: 316313].
[36] J.-Q. Liu, G.-M. Luo, X.-J. Ren, Y. Mu, Y. Bai, J.-C. Shen, *Biochim. Biophys. Acta* **2000**, *1481*, 222–228.
[37] X.-J. Ren, J.-Q. Liu, G.-M. Luo, Y. Zhang, Y.-M. Luo, G.-L. Yan, J.-C. Shen, *Bioconjugate Chem.* **2000**, *11*, 682–687.
[38] Y. Zhao, X.-Q. Liu, H.-Y. Zhu, Z.-M. Yang, R. Huang, *Chin. Chem. Lett.* **2006**, *17*, 1543–1546.
[39] Y. Zhao, Z.-M. Yang, H.-Y. Zhu, J. Gu, Y.-F. Wang, Wuli Huaxue Xuebao (*Acta Phys. Chim. Sin.*) **2007**, *23*, 394–398 (in Chinese) [AN 2007: 336390].
[40] Y. Liu, Y. Chen, L. Li, B. Li, H.-Y. Zhang, *Supramol. Chem.* **2002**, *14*, 299–307.
[41] Y. Liu, Y.-W. Yang, Y. Zhao, L. Li, H.-Y. Zhang, S.-Z. Kang, *J. Inclusion Phenom. Macrocyclic Chem.* **2003**, *47*, 155–160.
[42] R. C. Petter, J. S. Salek, C. T. Sikorski, G. Kumaravel, F.-T. Lin, *J. Am. Chem. Soc.* **1990**, *112*, 3860–3868.
[43] D. A. Lightner, J. E. Gurst, *Organic conformational Analysis and Stereo-Chemistry from Circular Dichroism Spectroscopy*, Wiley-VCH, New York, **2000**.
[44] M. Kajtar, C. Horvath-Toro, E. Kuthi, J. Szejtli, *Acta Chim. Acad. Sci. Hung.* **1982**, *110*, 327–355.

[45] K. Harata, H. Uedaira, *Bull. Chem. Soc. Jpn* **1975**, *48*, 375–378.
[46] M. Kodaka, *J. Am. Chem. Soc.* **1993**, *115*, 3702–3705.
[47] C. A. Haskard, C. J. Easton, B. L. May, S. F. Lincoln, *J. Phys. Chem.* **1996**, *100*, 14457–14461.
[48] B. Zhang, R. Breslow, *J. Am. Chem. Soc.* **1997**, *119*, 1676–1681.
[49] Y. Liu, Z.-Y. Duan, Y. Chen, J.-R. Han, L. Cui, *Org. Biomol. Chem.* **2004**, *2*, 2359–2364.
[50] Y. Liu, Y.-W. Yang, Y. Chen, F. Ding, *Bioorgan. Med. Chem.* **2005**, *13*, 963–971.
[51] Y. Liu, H.-M. Yu, Y. Chen, Y.-L. Zhao, *Chem. Eur. J.* **2006**, *12*, 3858–3868.
[52] Y. Liu, Y. Chen, B. Li, T. Wada, Y. Inoue, *Chem. Eur. J.* **2001**, *7*, 2528–2535.
[53] Y. Liu, C.-C. You, Y. Chen, T. Wada, Y. Inoue, *J. Org. Chem.* **1999**, *64*, 7781–7787.